

Mode Coupling for Phonons in a Single-Layer Dusty Plasma Crystal

Bin Liu, J. Goree, and Yan Feng

Department of Physics and Astronomy, The University of Iowa, Iowa City, Iowa 52242, USA

(Received 14 May 2010; published 20 August 2010)

New modes in a dusty plasma result from coupling of differently polarized phonons. A single horizontal layer of charged microparticles, confined so that vertical as well as horizontal motions are possible, usually exhibits three modes. An experiment shows that mode coupling leads to a new hybrid mode and another new mode. Coupling also leads to a recently reported hybrid mode and nondispersive mode, shown here to occur in an unmelted lattice. A linear theory based on ion wakes is able to predict some, but not all, of these modes. Other multiphase systems could exhibit similar mode coupling.

DOI: [10.1103/PhysRevLett.105.085004](https://doi.org/10.1103/PhysRevLett.105.085004)

PACS numbers: 52.27.Lw, 05.40.-a, 52.27.Gr

Dusty plasma consists of charged microparticles dispersed in an ionized gas. As in other multiphase systems such as colloids, the microparticles in dusty plasma can self-organize. Because they have a large charge and are confined, self-organization can result in a crystalline structure [1,2], which exhibits phonons [3,4]. Here we expand what was previously known about “mode coupling,” which is a modification of the phonon modes in a dispersed phase, enhanced by a flow in a continuous phase.

Observing this mode-coupling phenomenon requires an experimental system with a flow (directed energy) in a continuous phase, and a dispersed phase that sustains multiple modes. Here, the term “mode” refers to an oscillation, or phonon. Random particle motions, for example, due to thermal fluctuations, can be decomposed into these modes. If collective effects are significant, the frequency ω of a mode usually varies with wave number k , but if ω is independent of k , we will term the mode “nondispersive.” Modes are distinguished by the direction of particle velocity with respect to wave propagation, which we term “polarization.” In a crystalline lattice, there are longitudinal acoustic (LA) and transverse acoustic (TA) modes. If the experimental system has a suspension of dispersed microparticles that fill only a single layer, it will also have a third mode: an out-of-plane transverse optical mode (TO). The TO mode is dominated by oscillatory motion in the vertical confining potential, which is characterized by a resonance frequency, ω_{res} [5]. (The wave number \mathbf{k} is in-plane for all three modes.) These three modes have been previously studied in simulations with a Yukawa interparticle potential and a parabolic confining potential in the out-of-plane z direction, for example [6–8].

An experimental system that meets these requirements is a single-layer suspension of microparticles levitated in a plasma, i.e., dusty plasma. Its microparticles move slowly enough, and are large enough, that videomicrography can be used to track their motion. In our experiment, the microparticles comprise a strongly coupled plasma, and they self-organize in a crystalline lattice. Ions in the plasma represent a continuous phase that flows past the microparticles due to an electric field.

Recently, in what was perhaps the first experimental demonstration of mode coupling for a multiphase system with a directed flow of a continuous phase, Couédel *et al.* [9] observed coupling of the LA and TO modes in a single-layer dusty plasma. The dispersion relations of the modes were greatly modified, especially with the appearance of the LA-TO hybrid mode. A hybrid mode can occur when the dispersion relations for two different modes with different polarizations happen to have the same frequency ω and wave number k . The corresponding particle motion has a mixture of two directions. In the experiment of Ref. [9], a suspension of charged microspheres was electrically confined in a single layer, and there was an ion flow perpendicular to the layer. In addition to the LA-TO hybrid mode, what we term the nondispersive (ND) mode also appeared in their reported spectra. Their analysis was largely centered on large-amplitude particle motion in an extreme case that leads to melting of the crystalline structure of the single layer.

Here, we will report observations of two additional modes in an experiment with a crystalline structure. These two modes have apparently not been reported or predicted previously: a longitudinal mode that we term the longitudinal optical (LO) mode, and a transverse mode for in-plane motion that appears to be a hybrid of the TA and ND modes which we term the TA-ND hybrid mode. In addition to these two main results, we also find that the LA-TO hybrid and ND modes observed recently in an unstable melted lattice [9] can also occur in our stable crystalline lattice.

A frictionless linear theory predicts that mode coupling can excite hybrid modes in a single-layer dusty plasma suspension [10–12]. Mode coupling can be greatly enhanced if a system is nonequilibrium, for example, when an external power supply drives an ion flow in a dusty plasma, leading to an ion wake downstream of each charged microsphere [13–16]. An ion wake has a localized accumulation of positive charge.

In the frictionless linear theory [10–12], the effects of ions and electrons are replaced by a screening length λ_D and a hypothetical positively charged point particle, which

is rigidly attached a distance d_i downstream of a negatively charged microsphere. Phonon modes are identified by an eigenvalue analysis of a dynamical matrix. (This matrix is a Fourier transform of a force constant matrix obtained by linearizing potentials between a micro-particles and numerous neighbors and point particles, ignoring gas friction.) For a given wave number k , there are two eigenvalues ω^2 , which can be identical. If they are complex, the mode is either unstable or damped. A dispersion relation is found by plotting ω vs k . Eigenvectors indicate velocity direction (polarization).

To illustrate the role of ion wakes, we sketch in Fig. 1 a simple calculation showing that a small vertical displacement of a microparticle in a single layer results in a horizontal net force applied to neighboring particles. The horizontal force is weaker (second order in the displacement) in the absence of a wake effect, but stronger (first order) with the wake effect. Thus, the coupling of horizontal and vertical motions associated with low amplitude waves, like these reported here, is most likely to be observed when there is a wake potential.

In the experiment, we used two high-resolution video cameras to measure both in-plane and out-of-plane motions precisely and simultaneously. A top-view camera, with a field of view (FOV) of $37 \times 23 \text{ mm}^2$, imaged the single layer in a horizontal x - y plane. A side-view camera, with a FOV of $18 \times 10 \text{ mm}^2$, imaged a cross section in the vertical x - z plane. Images of $1152 \times 720 \text{ pixel}^2$ were recorded at 10 ms intervals for 50 s.

Our multiphase system consisted of $8.09 \mu\text{m}$ melamine formaldehyde polymer microspheres introduced into an rf plasma. A dc self-bias of -57 V drove a steady ion flow toward a horizontal lower electrode. More than 15 000 micro-particles were levitated in a single horizontal layer 8 mm above the electrode. (With only one layer, our system is not expected to exhibit modes peculiar to bilayer systems [4].) Micro-particles self-organized in a crystallinelike lattice, Figs. 2(a) and 2(b). An additional phase was neutral

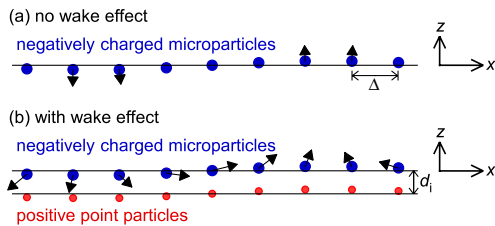


FIG. 1 (color online). Vectors for forces acting on micro-particles, calculated for two simple cases. (a) No ion-wake effect: micro-particles, with negative charge Q , interact only with nearest neighbors via a Yukawa potential. (b) With ion-wake effect: micro-particles also interact with a point particle with positive charge q_i located a distance d_i below the neighboring micro-particles. In these calculations, micro-particles are assumed to be disturbed vertically, but not horizontally, with a sinusoidal amplitude. Parameters assumed were $\Delta/\lambda_D = 1.0$, $q_i = -0.5Q$, and $d_i = 0.5\Delta$.

argon gas at 20 mtorr, which interacts with the micro-particles by exerting a frictional force. The damping rate, 3.5 s^{-1} , was low enough that the modes reported here were not overdamped.

For this experiment, it is important that the suspension be a nearly flat horizontal layer, without significant curvature. If it were curved, an out-of-plane velocity would have a horizontal vector component that our cameras would misidentify as being in-plane. In a test, we found that our suspension was planar to less than 0.03 rad, so that the fractional error in the energy in the spectrum will be negligible, $<(0.03)^2$.

We performed a main experiment that had stronger interparticle interactions ($\kappa \equiv b/\lambda_D = 0.9$) and a control experiment with less strong interactions ($\kappa = 1.4$). This was accomplished by introducing more particles into the plasma to achieve a smaller particle spacing for the main experiment. The lattice constant was $b = 0.6 \text{ mm}$ and 1.0 mm for the main and control experiments, respectively. Both experiments had the same conditions for gas, ions, electrons, screening length, and confining potentials. In both experiments, the collection of micro-particles comprised a strongly coupled plasma.

Our results are measurements of phonon spectra [5] for three polarizations, corresponding to random particle motion in the in-plane \hat{x} and \hat{y} directions, and the out-of-plane \hat{z} direction. The analysis begins with measuring micro-particle positions and velocities in each video frame [17]. Choosing a wave number k in the in-plane \hat{x} direction, we compute the longitudinal particle current $j_x(k, t) = \sum v_{x,i}(t)e^{-ikx_i(t)}$ using position x_i and velocity $v_{x,i}$ data from the top-view camera. Similarly, we find the transverse particle currents, $j_y(k, t) = \sum v_{y,i}(t)e^{-ikx_i(t)}$ and $j_z = \sum v_{z,i}(t)e^{-ikx_i(t)}$, using x_i and $v_{y,i}$ from the top-view camera, or x_i and $v_{z,i}$ from the side-view camera. The phonon spectrum (a graph of energy as a function of k and ω) is

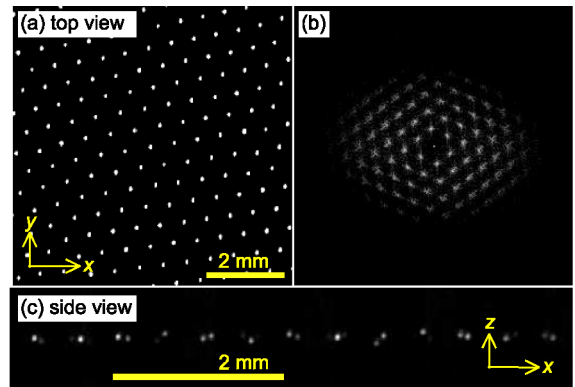


FIG. 2 (color online). (a) A portion of an image from the top-view camera, which was used to compute (b) the static structure factor [19]. Both show a crystalline structure. (c) Image from the side-view camera. These images are from the main experiment, with a lattice constant $b = 0.6 \text{ mm}$. The control experiment was similar, but with $b = 1.0 \text{ mm}$.

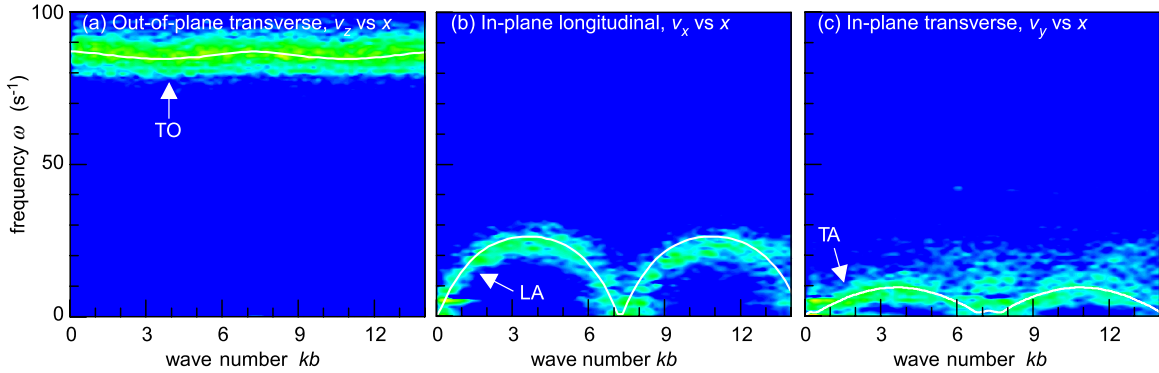


FIG. 3 (color online). Control experiment with $\kappa = 1.4$. Phonon spectra are shown for three polarizations (v_z , v_x , and v_y , all for \mathbf{k} in the \hat{x} direction). We can identify one mode for each polarization: (a) out-of-plane transverse (TO), (b) in-plane longitudinal (LA), and (c) in-plane transverse (TA). Smooth curves are dispersion relations calculated from a frictionless linear theory with no ion-wake effect, where we assumed that \mathbf{k} points 30° from \hat{x} .

then computed using the Fourier transformation of the particle currents. Values of ω and k that have significant energy describe a dispersion relation.

In our control experiment, we verified that without very strong interparticle interactions, signatures of mode coupling are lacking. Only the TO, LA, and TA modes are observed, Fig. 3. The TO mode's frequency $\sim 87 \text{ s}^{-1}$ is mainly due to the vertical confinement resonance at ω_{res} . The LA and TA modes have much lower frequencies determined more by interparticle interactions than by confining potentials. Their dispersion relations never cross that of the TO mode, as would be required for hybrid mode excitation. This control experiment also allowed us to determine the microparticle charge $Q = -9000e$ and $\lambda_D = 0.7 \text{ mm}$ using the method of [3]; these values also apply to the main experiment.

In our main experiment, which had the same confining potentials but stronger interparticle interactions, the spectra are profoundly different from those of the control experiment. At least four additional modes appear in the spectra, Figs. 4(a)–4(c); two of them were recently observed [9], and the others are new.

The two modes seen in our main experiment that were recently observed by Cou edel *et al.* [9] are indicated in italics in Figs. 4(a)–4(c); the first is the LA-TO hybrid mode. It occurs at the intersection of the dispersion relations of the LA and TO modes, i.e., at $kb \approx 2.6$ and $\omega \approx 58 \text{ s}^{-1}$, in Figs. 4(a) and 4(b). The hybrid mode has a mixture of v_x and v_z motions, as indicated by its appearance in both panels (a) and (b) of Fig. 4. This mode has an unusually large portion of the particle kinetic energy [see Figs. 4(d) and 4(e) at $kb \approx 2.6$].

The second mode that appeared in the spectra observed by Cou edel *et al.* [9], but not named or discussed in detail in [9], is what we term the ND mode. In our experiment, this mode appears at a constant frequency $\omega \approx 58 \text{ s}^{-1}$, independent of k , in Figs. 4(a)–4(c). This frequency is below $\omega_{\text{res}} \approx 87 \text{ s}^{-1}$. The ND mode involves particle motion in all three directions. Because this mode's ω and k are

not on the dispersion relations of any modes predicted by the model [12], its appearance must be due to an effect that is not included in the model (such as nonlinearity [9], gas friction, imperfections in the suspension, or ion-wake features ignored by the single-point-particle model). In the experiment, we also observed the second harmonic of the ND mode at 116 s^{-1} , suggesting nonlinearity.

The first new mode we observed is a longitudinal optical (LO) mode, for the polarization with microparticle motion in the \hat{x} direction. This new LO mode, in Fig. 4(b), has the same polarization as the typical LA mode, but a much higher frequency at small wave numbers. This new LO mode has negative dispersion, i.e., ω diminishes with k , and its dispersion relation coincides with that of the TO mode. Because the latter mode has motion in the \hat{z} direction, this LO mode appears to be the result of horizontal motion coupling with the vertical motion associated with the TO mode. This coupling is linear, because nonlinear coupling would likely result in a frequency or wave number that is different from the existing TO mode. (We verified that the energy of our LO mode is too high for the LO mode to be explained merely as a misidentification of the TO mode due to suspension curvature.)

The second new mode we observed is an in-plane transverse hybrid mode, for the polarization with microparticle motion in the \hat{y} direction. This new hybrid mode, in Fig. 4(c), appears at the intersection of the TA and non-dispersive (ND) modes. Thus, we interpret it as a hybrid of the TA and ND modes. This new TA-ND hybrid mode has an unusually large portion of kinetic energy for in-plane motion, Fig. 4(f), but not out-of-plane motion, Fig. 4(d).

We now compare the ω vs k dispersion relations of the two new modes with the smooth curves in Figs. 4(a)–4(c) predicted by the frictionless linear theory of [12]. We find that the new LO mode, but not the new TA-ND hybrid mode, are branches of the dispersion relation predicted by the theory [12]. We also find that the eigenvectors indicate a mixture of v_x and v_z motion for the LO mode (and for the LA-TO hybrid mode, as well).

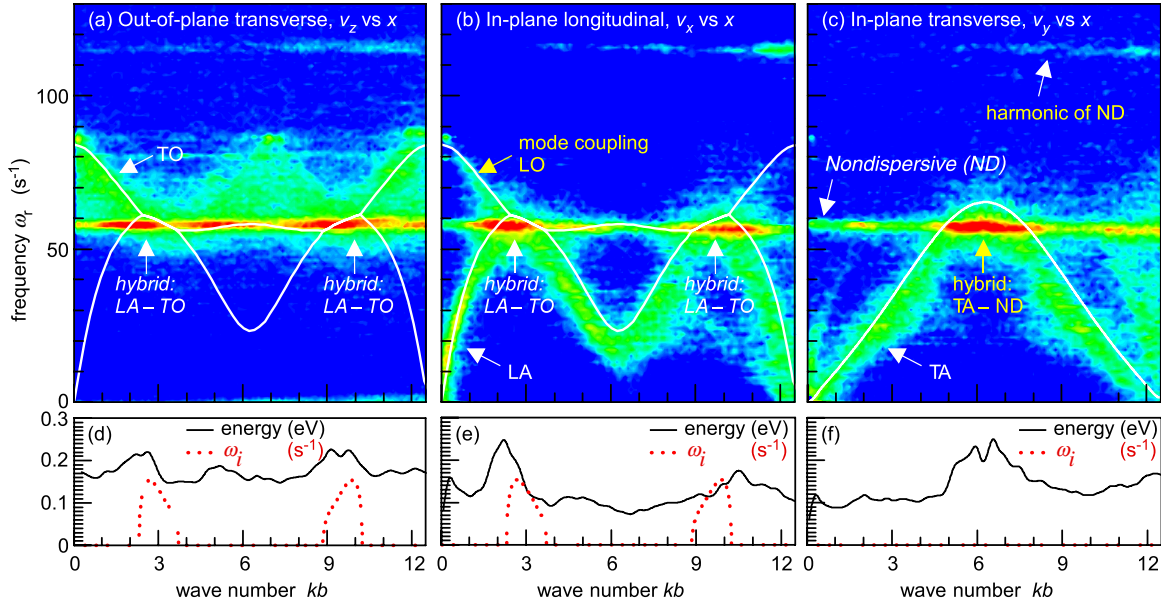


FIG. 4 (color online). Main experiment with a stronger interparticle interaction ($\kappa = 0.9$). The frequency of the TO mode overlaps with those for the LA and TA modes, leading to additional modes. The modes we term LA-TO hybrid and nondispersive (ND) modes were recently observed [9]. New modes found here are the longitudinal optical (LO) mode seen in (b) for $\omega > 58 \text{ s}^{-1}$ and $0 < kb < 3$, and the TA-ND hybrid mode seen in (c) for $kb = 6$ and $\omega = 58 \text{ s}^{-1}$. The smooth curves are the real parts of dispersion relations calculated from the frictionless linear theory, assuming Q and κ values from our control experiment, with ion-wake effects modeled as in Ref. [12]. All modes have real frequencies except for the LA-TO hybrid mode, which has both unstable and damped propagating solutions, $\omega_r \pm i\omega_i$. To achieve a fit, we adjusted these free parameters: $q_i = -0.7Q$ and $d_i = 0.7 \text{ mm}$, where we assumed that \mathbf{k} points 0° from \hat{x} . Energy for random motion (d), (e), and (f) is not equally partitioned among wave numbers: the hybrid modes consume much of the energy. The linear theory predicts the LA-TO mode has an unstable branch, as indicated by the dashed curves, with a growth rate ω_i that is weaker than the gas damping rate of 3.5 s^{-1} . Panels (a)–(c) use the same scale for wave energy; this scale is doubled as compared to Fig. 3.

This comparison indicates that all the required physics for the LO and LA-TO modes are present in the frictionless linear theory, but not for the TA-ND hybrid mode. Some physics, such as nonlinearity, must be lacking from the model because it fails to predict the TA-ND hybrid mode, the ND mode itself, and its harmonic.

Our results also demonstrate that hybrid modes resulting from mode coupling do not always cause melting. They also occur in our crystal, which was observed to be stable. This result should be compared to previous experiments [9,18], which indicated that high-amplitude motion associated with hybrid modes can melt a lattice. We conclude that melting is not an inevitable consequence of mode coupling.

In summary, we observed new modes: the LO mode which results from mode coupling, and the TA-ND hybrid mode which occurs at the intersection of the dispersion relations of the TA and ND modes. We confirmed that the previously observed ND and LA-TO hybrid modes can occur in stable crystalline lattices, without melting. A simple frictionless linear theory based on the ion-wake effect [12] cannot explain the ND and TA-ND modes.

We thank F. Skiff for helpful discussions. This work was supported by NSF and NASA.

- [1] J.H. Chu and L. I, *Phys. Rev. Lett.* **72**, 4009 (1994).
- [2] H. Thomas *et al.*, *Phys. Rev. Lett.* **73**, 652 (1994).
- [3] S. Nunomura *et al.*, *Phys. Rev. Lett.* **89**, 035001 (2002).
- [4] P. Hartmann *et al.*, *Phys. Rev. Lett.* **103**, 245002 (2009).
- [5] B. Liu *et al.*, *Phys. Plasmas* **16**, 083703 (2009).
- [6] K. Qiao and T.W. Hyde, *Phys. Rev. E* **68**, 046403 (2003).
- [7] Z. Donkó, P. Hartmann, and G.J. Kalman, *Phys. Rev. E* **69**, 065401(R) (2004).
- [8] Z. Donkó, G.J. Kalman, and P. Hartmann, *J. Phys. Condens. Matter* **20**, 413101 (2008).
- [9] L. Couëdel *et al.*, *Phys. Rev. Lett.* **104**, 195001 (2010).
- [10] A.V. Ivlev and G. Morfill, *Phys. Rev. E* **63**, 016409 (2000).
- [11] A.V. Ivlev *et al.*, *Phys. Rev. E* **68**, 026405 (2003).
- [12] S.K. Zhdanov, A.V. Ivlev, and G.E. Morfill, *Phys. Plasmas* **16**, 083706 (2009).
- [13] S.V. Vladimirov and M. Nambu, *Phys. Rev. E* **52**, R2172 (1995).
- [14] F. Melandsø and J. Goree, *Phys. Rev. E* **52**, 5312 (1995).
- [15] A. Melzer, V.A. Schweigert, and A. Piel, *Phys. Rev. Lett.* **83**, 3194 (1999).
- [16] A. Melzer *et al.*, *Phys. Rev. E* **54**, R46 (1996).
- [17] Y. Feng, J. Goree, and B. Liu, *Rev. Sci. Instrum.* **78**, 053704 (2007).
- [18] T.E. Sheridan, *Phys. Plasmas* **15**, 103702 (2008).
- [19] V. Nosenko and J. Goree, *Phys. Rev. Lett.* **93**, 155004 (2004).